Available online at www.sciencedirect.com
ScienceDirect
Journal of Power Sources 176 (2008) 306–311
JOURNAL OF POWER SOURCES
www.elsevier.com/locate/jpowsour

Short communication

Pt and Ru dispersed on $LiCoO_2$ for hydrogen generation from sodium borohydride solutions

Zhaolin Liu [a,*], Bing Guo [a], Siew Hwa Chan [b,c], Ee Ho Tang [d], Liang Hong [a]

[a] *Institute of Materials Research and Engineering of Singapore, 3 Research Link, Singapore 117602, Singapore*
[b] *SERC Fuel Cell Programme, Agency for Science, Technology and Research, 30 Biopolis Street, Singapore 138671, Singapore*
[c] *Fuel Cell Strategic Research Programme, School of Mechanical and Aerospace Engineering, Nanyang Technological University, 50 Nanyang Avenue, Singapore 639798, Singapore*
[d] *Directorate of Research and Development, Defence Science & Technology Agency, 1 Depot Road, Singapore 109679, Singapore*

Received 3 July 2007; accepted 24 September 2007
Available online 13 October 2007

Abstract

Nano-sized platinum and ruthenium dispersed on the surface $LiCoO_2$ as catalysts for borohydride hydrolysis are prepared by microwave-assisted polyol process. The catalysts are characterized by transmission electron microscopy (TEM), X-ray diffractometry (XRD) and X-ray photoelectron spectroscopy (XPS). Very uniform Pt and Ru nanoparticles with sizes of <10 nm are dispersed on the surface of $LiCoO_2$. XRD patterns show that the Pt/$LiCoO_2$ and Ru/$LiCoO_2$ catalysts only display the characteristic diffraction peaks of a $LiCoO_2$ crystal structure. Results obtained from XPS analysis reveal that the Pt/$LiCoO_2$ and Ru/$LiCoO_2$ catalysts contain mostly Pt(0) and Ru(0), with traces of Pt(IV) and Ru(IV), respectively. The hydrogen generation rates using low noble metal loading catalysts, 1 wt.% Pt/$LiCoO_2$ and 1 wt.% Ru/$LiCoO_2$, are very high. The hydrogen generation rate using Ru/$LiCoO_2$ as a catalyst is slightly higher compared with that of Pt/$LiCoO_2$.

Keywords: Sodium borohydride; Hydrogen generation; Platinum; Ruthenium; Lithium cobalt oxide, Proton exchange membrane fuel cell

1. Introduction

Proton exchange membrane fuel cell (PEMFC) using hydrogen as a fuel is considered to be a promising alternative to internal combustion engines due to its zero/low emissions. In order to operate a PEMFC successfully, a safe and convenient hydrogen storage and production system with a high hydrogen-storage density needs to be developed. A stabilized aqueous solution of sodium borohydride is a safe, simple and compact source of high-purity hydrogen. Schlesinger et al. [1] have reported that alkaline borohydride solutions undergo hydrolysis in the presence of various transition metal catalysts to produce hydrogen. Based on this, various catalysts such as Pt, Ru, Ni, Co, Co–P, Co–B, etc. have been developed for hydrogen production from borohydride solutions [2–12]. When sodium borohydride is used for generation of hydrogen, a rapid reaction is desired. Kojima et al. [3] reported that hydrogen generation can be accelerated by metal–metal oxide (Pt/CoO and Pt/$LiCoO_2$) catalysts prepared by the conventional impregnated method. It is well known that the catalytic activity of the metal is strongly dependent on the particle shape, size and size distribution. Conventional preparation techniques based on wet impregnation and chemical reduction of the metal precursors often do not provide adequate control of particle shape and size. There are continuing efforts to develop alternative synthesis methods based on microemulsions, sonochemistry, microwave irradiation and catalytic organic reaction, which are more conducive to generating nanoscale colloids or clusters with better uniformity.

The polyol process, in which an ethylene glycol solution of the metal precursor salt is slowly heated to produce colloidal metal, has recently been extended to produce metal nanoparticles supported on carbon and Al_2O_3 [13–15]. In the process, the polyol solution containing the metal salt is refluxed at 393–443 K to decompose ethylene glycol to yield, in situ, a species for the reduction of the metal ions to their elemental states. The fine metal particles so produced may additionally be captured by a support material suspended in the solution. Conductive heating is often used, but microwave dielectric loss heating may be a

* Corresponding author. Tel.: +65 68727532; fax: +65 68720785.
E-mail address: zl-liu@imre.a-star.edu.sg (Z. Liu).

0378-7753/$ – see front matter © 2007 Elsevier B.V. All rights reserved.
doi:10.1016/j.jpowsour.2007.09.114

better synthesis option in view of its energy efficiency, speed, uniformity, and simplicity of implementation [16].

In this paper, Pt/$LiCoO_2$ and Ru/$LiCoO_2$ catalysts are prepared by a simple microwave-assisted polyol procedure for obtaining Pt and Ru nanoparticles and then tested for hydrogen generation. The crystal structure and activity for borohydride hydrolysis of the resulting catalysts are investigated.

2. Experimental

2.1. Chemicals

Hydrogen hexachloroplatinate hydrate, ruthenium chloride, sodium hydroxide and sodium borohydride were obtained from Aldrich and used as-received. Ethylene glycol (EG) was purchased from Mallinckrodt, AR. $LiCoO_2$ (lithium cobalt oxide, SC10) was received from Merck. All aqueous solutions were prepared using distilled water.

2.2. Preparation of Pt/$LiCoO_2$ and Ru/$LiCoO_2$ catalysts

In a 50 mL beaker, 1.28 mL of an aqueous solution of 20 mM $H_2PtCl_6{\cdot}6H_2O$ or 2.48 mL of an aqueous solution of 20 mM $RuCl_3$ was mixed with 30 mL of ethylene glycol. 0.495 g of $LiCoO_2$ were added and sonicated. The beaker and its contents were heated in a microwave oven (National NN-S327WF, 2450 MHz, 700 W) for 40 s. The resulting suspension was filtered. The residue was washed with water and acetone and then dried at 100 °C over night in a vacuum oven. Pt/$LiCoO_2$ and Ru/$LiCoO_2$ composites with amount 1 wt.% Pt or 1 wt.% Ru were obtained.

2.3. Characterizations

The particle morphology and size of the Pt and Ru were characterized by transmission electron microscopy (TEM) using a JEOL JEM 2010 system operating at 300 kV. For microscopic examination, the samples were first ultrasonicated in acetone for 1 h and then deposited on 3-mm Cu grids covered with a continuous carbon film. To determine the actual platinum and ruthenium contents, inductively coupled plasma spectroscopy (ICP) was used to measure the unreacted metal ions remaining in the ethylene glycol–water mixtures. Crystalline structures of the powders were characterized by XRD on a Bruker GADDS diffractometer using Cu Kα radiation and a graphite monochromator (the accelerating voltage and the applied current were 40 kV and 40 mA, respectively). X-ray photoelectron spectroscopy (XPS) analyses of the samples were performed on a VG ESCALAB MKII spectrometer. Narrow-scan photoelectron spectra of Pt4f and Ru3p were recorded. Peak deconvolution was performed using the curve-fitting program VGX900.

2.4. Hydrogen generation

Hydrogen generation was performed with a thermostatted glass vessel system. The catalysts were placed in a reactor prior to the hydrogen generation reaction. The system was sealed and pure nitrogen gas was fed into the system for purging the air. A thermocouple was also inserted through the septum to measure the temperature. $NaBH_4$–NaOH solution was pumped from a storage tank to the reactor, and the catalytic hydrolysis reaction was processed continuously on the catalyst bed. The generated hydrogen was channelled into a special bottle to clean up the residual alkali. The generated volume of hydrogen was measured using a mass-flow meter.

3. Results and discussion

3.1. Characterization of Pt/$LiCoO_2$ and Ru/$LiCoO_2$ catalysts

Platinum and ruthenium nanoparticles were prepared and directly deposited on to the $LiCoO_2$ surface by microwave heating of ethylene glycol solutions of platinum and ruthenium salts. Fig. 1 presents TEM images of the Pt/$LiCoO_2$ and Ru/$LiCoO_2$ catalysts. The surface of both catalysts is decorated with nano-sized Pt or Ru particles (<10 nm), which show a remarkably

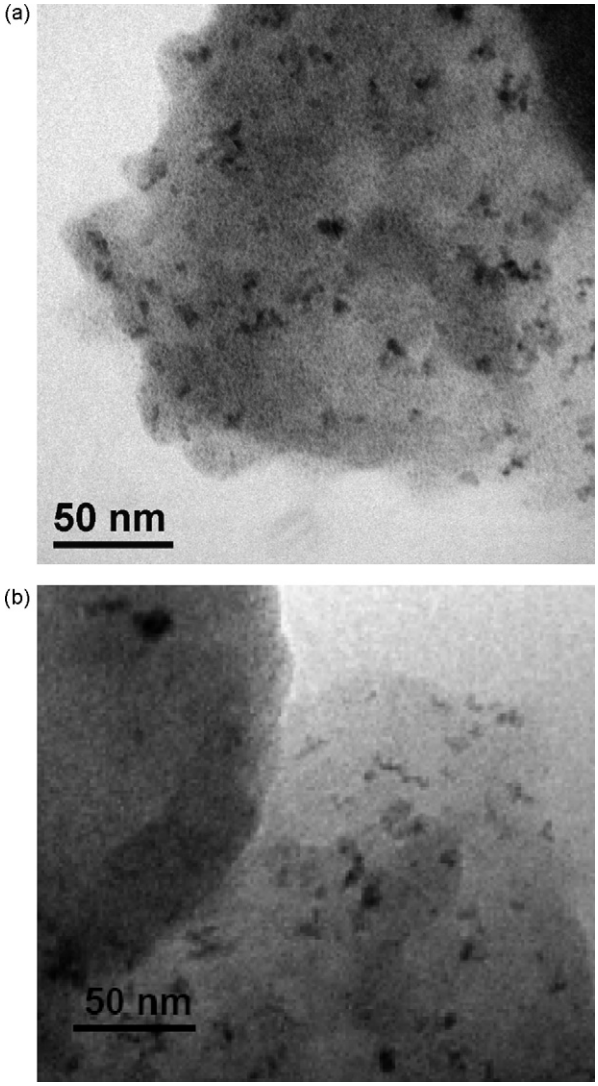

Fig. 1. TEM images of Pt/$LiCoO_2$ (a) and Ru/$LiCoO_2$ (b) catalysts.

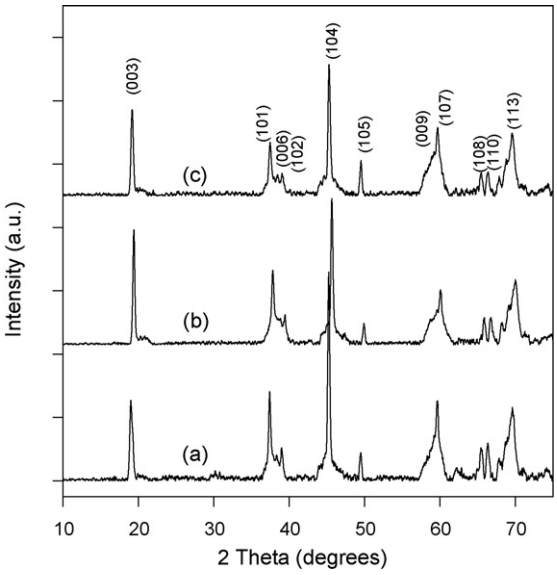

Fig. 2. XRD patterns of $LiCoO_2$ (a), Pt/$LiCoO_2$ (b) and Ru/$LiCoO_2$ (c) catalysts.

uniform and high dispersion of metal particles on the $LiCoO_2$ surface. This is similar to our previous studies on preparing Vulcan carbon and carbon nanotubes supported PtRu particles by a microwave-assisted polyol process [13,14]. The microwave-assisted heating of H_2PtCl_6 in ethylene glycol has evidently facilitated the formation of smaller and more uniform dispersion of Pt or Ru particles on either the $LiCoO_2$ surfaces. It is generally agreed that the size of metal nanoparticles is determined by the rate of reduction of the metal precursor. The dielectric constant (41.4 at 298 K) and the dielectric loss of ethylene glycol are high, and hence rapid heating occurs easily under microwave irradiation. In ethylene glycol mediated reactions (the 'polyol' process), ethylene glycol also acts as an agent to reduce the metal ion to metal powders. The fast heating by microwave accelerates the reduction of the metal precursor and the nucleation of the metal clusters. The easing of the nucleation-limited process greatly assists the formation of small particles. Additionally, the homogeneous microwave heating of liquid samples reduces the temperature and concentration gradients in the reaction medium, thus providing a more uniform environment for the nucleation and growth of metal particles. The $LiCoO_2$ surface may contain sites suitable for heterogeneous nucleation and the presence of a $LiCoO_2$ surface interrupts particle growth. The smaller and nearly single dispersed Pt or Ru nanoparticles on $LiCoO_2$ prepared by microwave irradiation can be rationalized in terms of these general principles.

ICP measurements show Pt contents of 0.97 wt.% for the Pt/$LiCoO_2$ and 0.93 wt.% for the Ru/$LiCoO_2$ prepared from the feeds of 1 wt.%.

Powder X-ray diffraction (XRD) patterns for the Pt/$LiCoO_2$ and the Ru/$LiCoO_2$ are shown in Fig. 2 alongside the diffraction patterns of the $LiCoO_2$ powder taken as a comparison. The patterns remain unchanged after Pt or Ru deposition on $LiCoO_2$, which suggests that Pt or Ru loading has modified only the surface of the $LiCoO_2$ without changing the crystal structure of the bulk material. Some characteristic peaks of rhombohedral $LiCoO_2$ ($2\theta = 19.1°$, 37.4°, 38.4°, 39.1°, 45.3°, 49.5°, 59.1°, 60.1°, 65.8°, 66.5° and 69.7°) that are associated with the (0 0 3), (1 0 1), (0 0 6), (0 1 2), (1 0 4), (1 0 5), (0 0 9), (1 0 7), (1 0 8), (1 1 0) and (1 1 3) reflections are observed in the 2θ range from 10° to 75° [17]. Additionally, no peaks for platinum (40.0° and 68.1°) and ruthenium (37.5° and 44.0°) are observed for the Pt/$LiCoO_2$ and the Ru/$LiCoO_2$ catalysts, which may be due to undetectable very low Pt or Ru loadings. No characteristic peaks of other impurities, such as CoO and Co_3O_4, are observed, which indicates that the $LiCoO_2$ has high purity.

The Pt4f and Ru3p regions of the XPS spectrum for the Pt/$LiCoO_2$ and Ru/$LiCoO_2$ catalysts, respectively, are presented in Fig. 3. The Pt4f region shows two doublets from the spin-orbital splitting of the $4f_{7/2}$ and $4f_{5/2}$ states. The main doublet at 71.0 and 74.3 eV is contributed by $Pt4f_{7/2}$, and can be used to indicate the presence of metallic platinum. A small doublet due to $Pt4f_{5/2}$ is detected at 72.4 and 75.7 eV, which demonstrates the presence of higher oxidation states of Pt, such as Pt(IV) (e.g., PtO_2) in the sample [18]. The slight shift in the Pt(0) peak to higher binding energies is a known effect for small particles, as reported by Roth et al. [19]. The Ru3p signal is deconvoluted into two distinguishable pairs of peaks of different intensities located at 460.7 and 464.6 eV, which correspond well with Ru(0) and RuO_2, respectively [20].

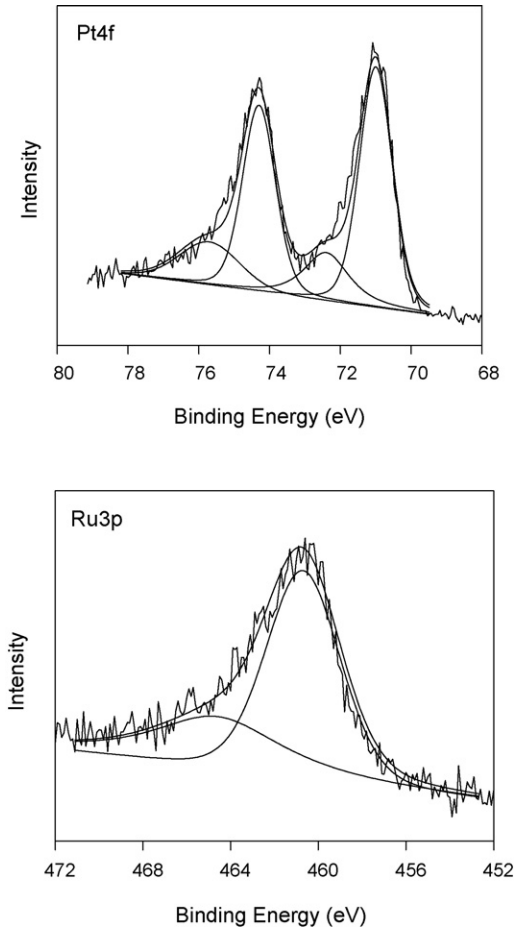

Fig. 3. X-ray photoelectron spectra of Pt/$LiCoO_2$ and Ru/$LiCoO_2$ catalysts.

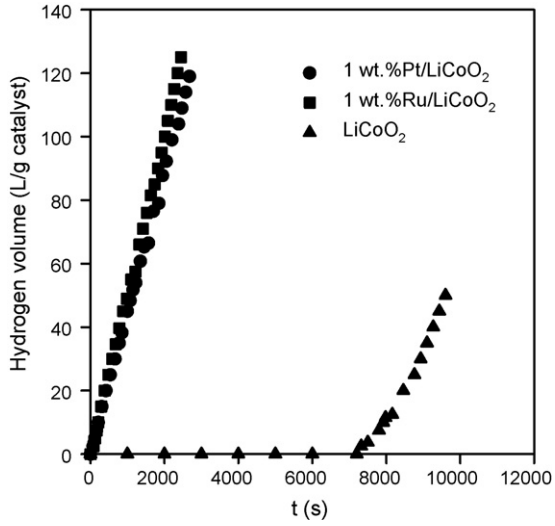

Fig. 4. H_2 generation rate at 25 °C using 20 mg of different catalysts in 10 mL of 10% $NaBH_4$ + 5% NaOH solution.

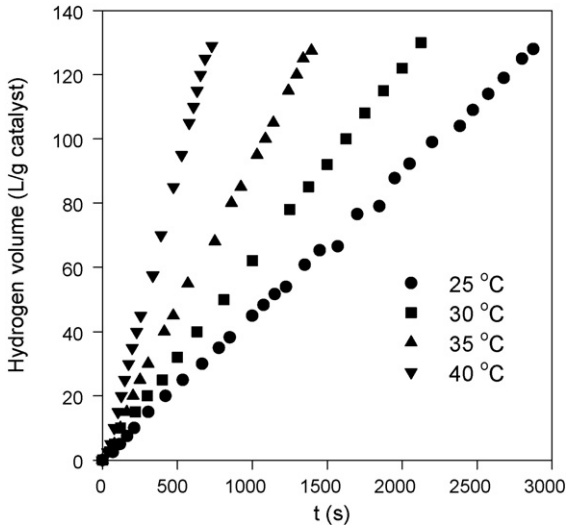

Fig. 5. Effects of solution temperature on hydrogen generation rate using 20 mg of 1 wt.% $Pt/LiCoO_2$ catalyst in 10 mL of 10% $NaBH_4$ + 5% NaOH solution.

3.2. Catalytic activity for borohydride hydrolysis

The hydrolysis reaction of $NaBH_4$ is shown as follows:

$$NaBH_4\,(37.8) + 2H_2O\,(36) \rightarrow 4H_2\,(8) + NaBO_2\,(65.8) \quad (1)$$

The cumulative volumes of hydrogen generation with time for the reaction of $NaBH_4$ with water using various catalysts are shown in Fig. 4. With pure $LiCoO_2$, the time required for the hydrolysis reaction to begin is about 2 h. With $Pt/LiCoO_2$ and $Ru/LiCoO_2$, the hydrolysis reaction starts immediately once the catalyst is in contact with the $NaBH_4$ solution. The cumulative volumes of hydrogen generation increase almost linearly with reaction time, which suggests that the reaction rates are unchanged as the hydrolysis reaction continues. Thus, the hydrogen generation rate can be expressed by the following zero-order rate equation

$$-\frac{1}{4}\frac{dc_{NaBH_4}}{dt} = \frac{dc_{H_2}}{dt} = k \quad (2)$$

where k is the rate constant for hydrogen generation and is 0.045 and 0.05 $L(H_2)\,(s\,g(catalyst))^{-1}$ for $Pt/LiCoO_2$ and $Ru/LiCoO_2$, respectively. The hydrogen generation rate using a $Ru/LiCoO_2$ catalyst is slightly higher than that of a $Pt/LiCoO_2$ catalyst. The k values using 1 wt.% $Pt/LiCoO_2$ and 1 wt.% $Ru/LiCoO_2$ catalysts are much higher than those reported by Amendola et al. [21].

The effects of reaction temperature on the hydrogen generation for $Pt/LiCoO_2$ are given in Fig. 5. According to the Arrhenius equation, the reaction rate constant can be written as follows:

$$k = k_0 \exp\left(-\frac{E_a}{RT}\right) \quad (3)$$

where k_0 is the pre-exponential parameter, E_a the activation energy of the reaction, R the gas constant, and T is the reaction temperature.

From the slope of ln k versus $1/T$ (Fig. 6), activation energies of various hydrogen generation reaction are calculated to be 70.4 kJ mol^{-1} for $Pt/LiCoO_2$ and 68.5 kJ mol^{-1} for $Ru/LiCoO_2$, which are very similar to the values obtained by Jeong et al. [22] and Kaufman and Sen [23].

The influence of $NaBH_4$ concentration on the rate of hydrogen generation at 25 °C using 20 mg of 1 wt.% $Ru/LiCoO_2$ catalyst is shown in Fig. 7. The hydrogen generation rate decreases when the $NaBH_4$ concentration is raised from 5 to 25 wt.%. These results are consistent with those of the previous researches [22,24]. It is reasonable to attribute these data to the increase of the solution viscosity with the increase of $NaBH_4$ concentration. The increase of the solution viscosity may cause mass-transport limitations of borohydride from the solution to the surface of catalyst.

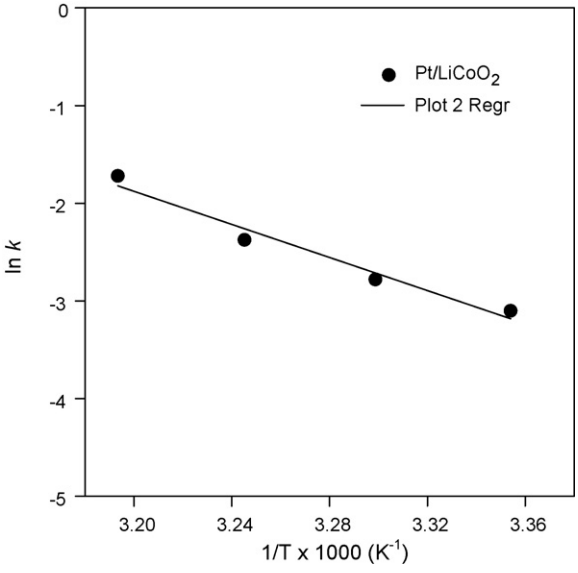

Fig. 6. Arrhenius plot for sodium borohydride hydrolysis using 20 mg of 1 wt.% $Pt/LiCoO_2$ catalyst in 10 mL of 10% $NaBH_4$ + 5% NaOH solution.

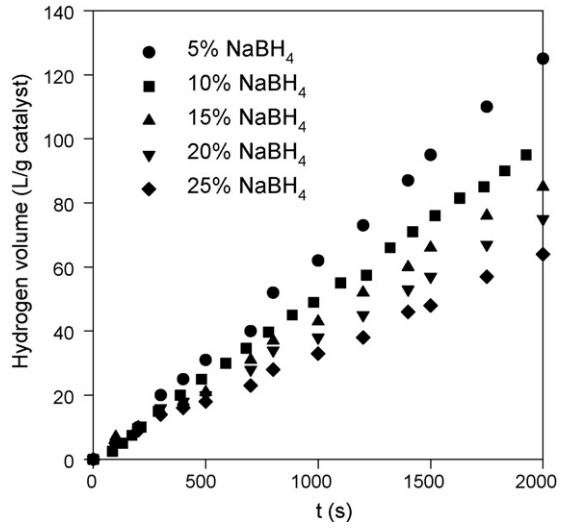

Fig. 7. Effects of $NaBH_4$ concentration on hydrogen generation rate at 25 °C using 20 mg of 1 wt.% $Ru/LiCoO_2$ catalyst in 10 mL of 5% NaOH solution.

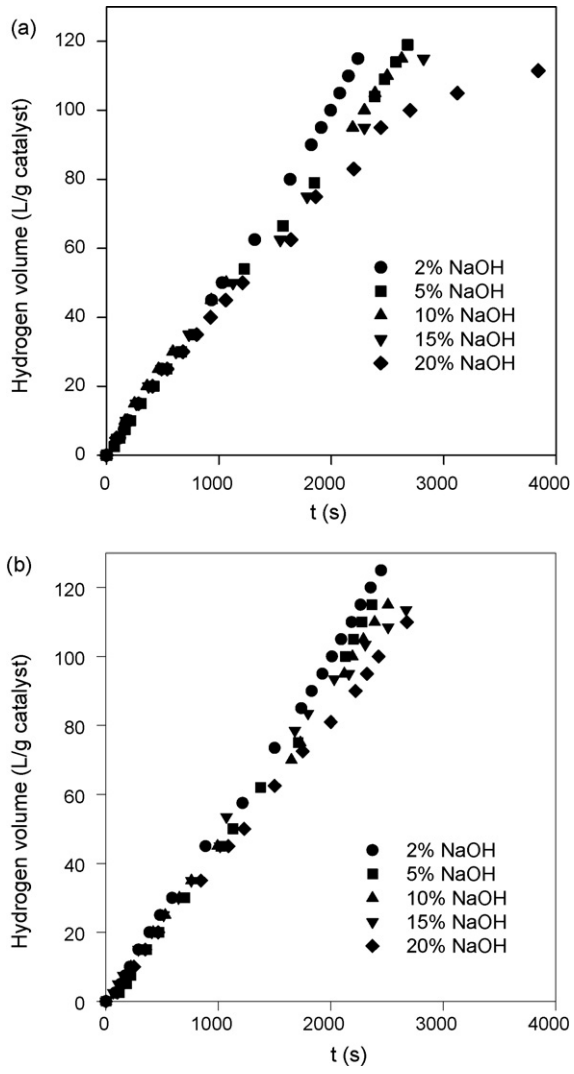

Fig. 8. Effects of NaOH concentration on hydrogen generation rate at 25 °C using 20 mg of 1 wt.% $Pt/LiCoO_2$ (a) and 1 wt.% $Ru/LiCoO_2$ (b) catalysts in 10 mL of 10% $NaBH_4$ solution.

The effect of NaOH concentration on the hydrogen generation rate at 25 °C using 20 mg of 1 wt.%$Pt/LiCoO_2$ and 1 wt.%$Ru/LiCoO_2$ catalysts is shown in Fig. 8. For both of the catalysts, hydrogen generation rate from $NaBH_4$ solution decreases slightly with increasing NaOH concentration, probably due to the reduced activity of water and lowered solubility of the reaction product $NaBO_2$ at higher NaOH concentration. These results are opposite to those obtained using Co–B [11], Co/Al_2O_3 [24] and Ni_xB [25] catalysts. It is well recognized that the self-hydrolysis of $NaBH_4$ takes place by the reaction of borohydride ions with protons dissociated from water. In alkaline solution, the slow self-hydrolysis of $NaBH_4$ is primarily due to the reduction of proton concentration and hydroxide ions act as an inhibitor for the catalyzed BH_4^- hydrolysis.

4. Conclusions

A microwave-assisted rapid heating method has been used to prepare $LiCoO_2$ powder supported Pt and Ru nanoparticles with high catalytic activities for hydrogen generation from $NaBH_4$ solution. The preparation method is simple, fast and energy efficient. The Pt and Ru nanoparticles (<10 nm) are uniformly dispersed on the surfaces of the $LiCoO_2$ particles. X-ray diffraction patterns show that the $Pt/LiCoO_2$ and $Ru/LiCoO_2$ catalysts only display the characteristic diffraction peaks of a $LiCoO_2$ crystal structure. Results obtained from XPS analysis reveal that the catalysts contain mostly Pt(0) and Ru(0), with traces of Pt(IV) and Ru(IV), respectively. The hydrogen generation rates using low loadings of the noble metals, i.e., 1 wt.% $Pt/LiCoO_2$ and 1 wt.% $Ru/LiCoO_2$, reach 0.045 and 0.05 $L(H_2)\,(s\,g(catalyst))^{-1}$, respectively, at 25 °C. With increasing solution temperature, rate of hydrogen generation increases and activation energies of the borohydride hydrolysis reaction are calculated to be 70.4 kJ mol^{-1} for $Pt/LiCoO_2$ and 68.5 kJ mol^{-1} for $Ru/LiCoO_2$, respectively. The rates decrease with increasing $NaBH_4$ concentration from 5 to 25 wt.% but decrease slightly with increasing NaOH concentration from 2 to 20 wt.%.

References

[1] H.I. Schlesinger, H.C. Brown, A.E. Finholt, J.R. Gilbreath, H.R. Hoekstra, E.K. Hyde, J. Am. Chem. Soc. 75 (1953) 215.
[2] H.C. Brown, C.A. Brown, J. Am. Chem. Soc. 84 (1962) 1493.
[3] Y. Kojima, K. Suzuki, K. Fukumoto, M. Sasaki, T. Yamamoto, Y. Kawai, H. Hayashi, Int. J. Hydrogen Energy 27 (2002) 1029.
[4] S.C. Amendola, S.L. Sharp-Goldman, M.S. Janjua, N.C. Spencer, M.T. Kelly, P.J. Petillo, M. Binder, Int. J. Hydrogen Energy 25 (2000) 969.
[5] C. Wu, H. Zhang, B. Yi, Catal. Today 93–95 (2004) 477.
[6] Z.T. Xia, S.H. Chan, J. Power Sources 152 (2005) 46.
[7] J.H. Kim, H. Lee, S.C. Han, H.S. Kim, M.S. Song, J.Y. Lee, Int. J. Hydrogen Energy 29 (2004) 263.
[8] P. Krishnan, T.H. Yang, W.Y. Lee, C.S. Kim, J. Power Sources 143 (2005) 17.
[9] A.M.F.R. Pinto, D.S. Falcao, R.A. Silva, C.M. Rangel, Int. J. Hydrogen Energy 31 (2006) 1341.
[10] K.W. Cho, H.S. Kwon, Catal. Today 120 (2007) 298.
[11] J. Lee, K.Y. Kong, C.R. Jung, E. Cho, S.P. Yoon, J. Han, T.G. Lee, S.W. Nam, Catal. Today 120 (2007) 305.
[12] J.H. Wee, K.Y. Lee, S.H. Kim, Fuel Process. Technol. 87 (2006) 811.

[13] W.X. Chen, J.Y. Lee, Z.L. Liu, Chem. Commun. (2002) 2588.
[14] Z.L. Liu, J.Y. Lee, W.X. Chen, M. Han, L.M. Gan, Langmuir 20 (2004) 181.
[15] A. Miyazaki, I. Balint, K.I. Aika, Y. Nakano, J. Catal. 203 (2001) 364.
[16] S.A. Galema, Chem. Soc. Rev. 26 (1997) 233.
[17] Powder Diffraction File, Database Manager T.M. Kahmer, Editor-in-Chief W.F. McClune, Editor of Calculated Patterns S.N. Kabekkodu, Staff Scientist H.E. Clark, International Certer for Diffraction Data (JCPDS), Pennsylvania USA, 2001.
[18] A.K. Shukla, M.K. Ravikumar, A. Roy, S.R. Barman, D.D. Sarma, A.S. Aricò, V. Antonucci, I. Pino, N. Giordano, J. Electrochem. Soc. 141 (1994) 1517.
[19] C. Roth, M. Goetz, H. Fuess, J. Appl. Electrochem. 31 (2001) 793.
[20] J.F. Moulder, W.F. Stickle, P.E. Sobol, K.D. Bomben, Handbook of X-ray Photoelectron Spectroscopy, Perkin Elmer, USA, 1992.
[21] S.C. Amendola, S.L. Sharp-Goldman, M.S. Janjua, N.C. Spencer, M.T. Kelly, P.J. Petillo, M. Binder, J. Power Sources 85 (2000) 186.
[22] S.U. Jeong, R.K. Kim, E.A. Cho, H.J. Kim, S.W. Nam, I.H. Oh, S.A. Hong, S.H. Kim, J. Power Sources 144 (2005) 129.
[23] C.M. Kaufman, B. Sen, J. Chem. Soc. Dalton Trans. (1985) 307.
[24] W. Ye, H. Zhang, D. Xu, L. Ma, B. Yi, J. Power Sources 164 (2007) 544.
[25] H. Dong, H. Yang, X. Ai, C. Cha, Int. J. Hydrogen Energy 28 (2003) 1095.